

Desulfurization of flue gases using materials based on $\text{Ca}(\text{OH})_2$ supported on clays

ABSTRACT

Acid rain is a worldwide environmental problem that started in industrialized countries, and it has been extended to underdeveloped countries. Actions must be taken, and one of those is to deal with one of the major SO_2 emission sources that are thermal power plants. A way of decreasing the SO_2 emissions is to treat the flue gases with sorbent materials, which selectively trap the SO_2 . These materials may be based on calcium and many efforts have been recently performed in order to increase their activity and yield. In the present work, SO_2 sorbent materials, based on $\text{Ca}(\text{OH})_2$ at different mass ratios, were prepared supported on clays (bentonite and tonsil), and their activity was tested in a thermogravimetric balance. In addition, ultrasonic energy was applied during preparation trying to improve their performance. It was found that activity increased proportional to the Ca load. Also, when temperature increased from 350 to 450°C, the SO_2 sorption capacity increased. The support clays did not play an important role; at low temperature, activity was slightly better in materials supported on tonsil, but as temperature increased the yield of materials supported on bentonite surpassed those of material supported on tonsil. Ultrasonic energy did not improve the performance of sorbent materials, and, in fact, the sorption capacity diminished when ultrasonic energy was applied during preparation of materials. Finally, the SO_2 sorption process was modeled using a modified shrinking core approach and kinetics parameters were estimated.

Keywords: acid rain, $\text{Ca}(\text{OH})_2$, tonsil, bentonite, sorbent materials, flue gas desulfurization, ultrasonic energy, kinetics parameter estimation

1. INTRODUCTION

The combustion of fossil fuel for the generation and/or transformation of energy in sectors, such as, industry, transport and commercial has caused an increase in the concentrations of gaseous and particulate pollutants in the atmosphere. This increase in pollutants has resulted in air pollution. One of the most critical environmental problems is the acid rain, which is a broad term that describes several ways through which acid falls out, including acidic rain, fog, hail and snow. At the beginning of the problem, acidic rainfall was commonly detected around industrial areas; however, with the increased use of tall stacks for power plants and industries, atmospheric emissions are now transported beyond the industrial areas. Acid rain is the result of many steps of chemical reactions between air borne pollutants (oxides of sulfur, nitrogen and other constituents present in the atmosphere) and atmospheric water and oxygen. Main sources of these oxides are fossil fuel fired power stations and smelters for SO_2 , and motor vehicle exhausts for NO_x . These oxides may react with other chemicals and produce corrosive substances that are washed out either in wet or dry form by rain as acid deposition [1-3].

Acid rain has several effects in the ecosystem, which include the decay in growth of trees, crops, aquatic flora and fauna. In addition, soil fertility is deteriorated as a result of leaching of nutrient cations and the increased availability of toxic heavy metals. Also, stones, metals, paints, textiles and ceramics can be eroded and corroded due to acid rain. It can also indirectly affect human health since it has been shown that SO_2 and NO_x contribute to the formation of $\text{PM}_{2.5}$ [3-6]. The acid rain problem has been tackled to some extent in developed countries by reducing the emission of the precursor gases, and several actions have been created in different parts of the world i.e., the Gothenburg

36 Protocol for the European Union and the US Acid Rain Program in the Title IV of the 1990 Clean Air
37 Act Amendments. [7-10].

38 Due to the rapid economic development and energy consumption throughout the world, fossil fuel
39 consumption has significantly increased during the last few decades. The use of fossil fuel is the
40 major cause of large-scale generation of acid precursors in the atmosphere. The problem was
41 originally identified as an issue in developed countries, but with the increase in industrialization and
42 urbanization, developing countries are now also experiencing this issue.

43 Many reviews have been published related to commercial and pilot-plant technologies for the
44 abatement of SO_2 from thermal power plants [11-13]. Most of the probed technologies are based in
45 calcium sorbents, such as, $\text{Ca}(\text{OH})_2$ and CaO , either in wet or dry conditions. New research efforts
46 have been addressed to improve the yield of calcium materials as SO_2 sorbent by mixing it with
47 several supports, such as, silica, fly ash, blast furnace slag, clays, and activated carbon [14-21]. In the
48 present work $\text{Ca}(\text{OH})_2$ was mixed with bentonite and tonsil at many mass ratios. These clays were
49 chosen because they are abundant in Mexico and can be considered a local low-cost raw material,
50 which would reduce the operating cost if they were applied in a local power plant. Bentonite is an
51 aluminiumhydrosilicate, in which the proportion of silicic acid to alumina is about 4:1. On the other
52 hand, tonsil is created from bentonite by acid activation. During this activation, the individual layers
53 are attacked by the acid; as result, aluminum, iron, calcium and magnesium ions are released from
54 the lattice. Also, in a way for further improvement the performance of the sorbent materials, ultrasonic
55 energy may be applied during preparation in an effort to reduce the particle size and increase
56 available active sites as it has occurred in other materials [22-26].

57

58

59 2. MATERIAL AND METHODS

60

61 2.1. Sorbent Preparation

62 Samples of $\text{Ca}(\text{OH})_2$ supported in bentonite and tonsil were synthesized by preparing slurries at
63 different mass ratio. Some of them were mechanically stirred during 4 h at 60-70°C. In other slurries,
64 ultrasonic energy was applied during 4 h maintaining the temperature below 70°C. After the mixing,
65 slurries were dried overnight a 120°C and pulverized.

66

67 2.2. Sorbent characterization

68 To determine the actual calcium content, samples of the sorbent-materials were analyzed by Atomic
69 Absorption Spectroscopy. Table 1 presents the composition of the different materials.

70

71

72 **Table 1. Calcium composition in the prepared sorbent materials.**

Material	$\text{Ca}(\text{OH})_2$ content [wt%]
Ca-Bentonite 1:2 MS	30.7505
Ca-Tonsil 1:2 MS	34.4440
Ca-Bentonite 1:1 MS	47.7199
Ca-Tonsil 1:1 MS	51.9835
Ca-Bentonite 2:1 MS	67.9053
Ca-Tonsil 2:1 MS	68.0212
Ca-Bentonite 1:2 UE	30.3809
Ca-Tonsil 1:2 UE	32.0253
Ca-Bentonite 1:1 UE	49.7233
Ca-Tonsil 1:1 UE	51.2866
Ca-Bentonite 2:1 UE	64.3171
Ca-Tonsil 2:1 UE	63.6533

73 MS: Mechanical Stirring

74 UE: Ultrasonic Energy

75

76

77 2.3. Sulfation of sorbents

78 The sulfation of the materials was carried out in a thermogravimetric balance (TA Instruments 2050)
79 by passing a stream of certified 3600 ppm_v SO₂/N₂ through a known amount of sorbent material. The
80 gas flow rate was 100 mL/min, which is the maximum flow of the thermobalance. The gain of weight in
81 the material was assigned to the sorption of SO₂ on the active sites.

82

83

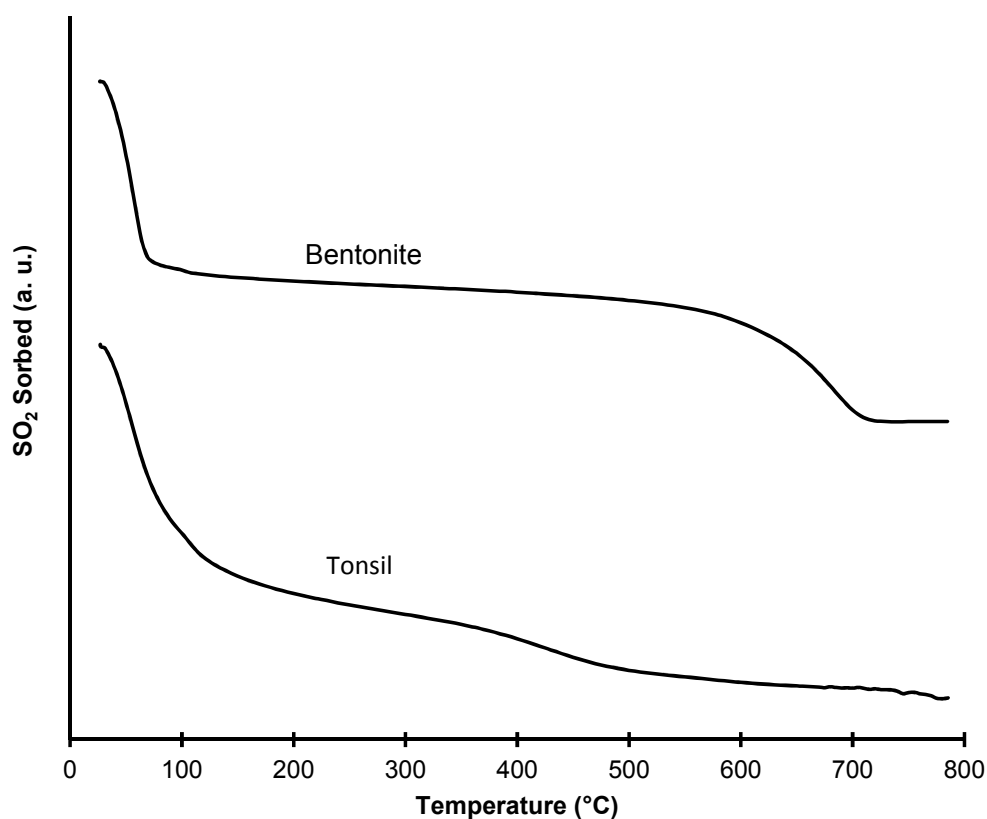
84 3. RESULTS AND DISCUSSION

85

86 3.1. Sorption of SO₂ on bentonite and tonsil

87 Experiments in the TGA varying temperature (heating rate: 10°C/min) were performed to check if
88 supports were able to adsorb SO₂. Results are presented in Fig. 1, and it was observed that none of
89 the clays retained SO₂. In fact, it was noticed that weight loss occurred as the temperature increased;
90 however, this is attributed to a loss of humidity in the interval between room temperature and 120°C.
91 Then, a drastic weight loss was observed, especially in bentonite, at temperatures higher than 550°C;
92 this is a result of the thermal rearrangement of the crystalline structure.

93



94

95 **Figure 1. Thermogravimetric profiles of the supports in the sulfurization process at variable**
96 **temperature.**

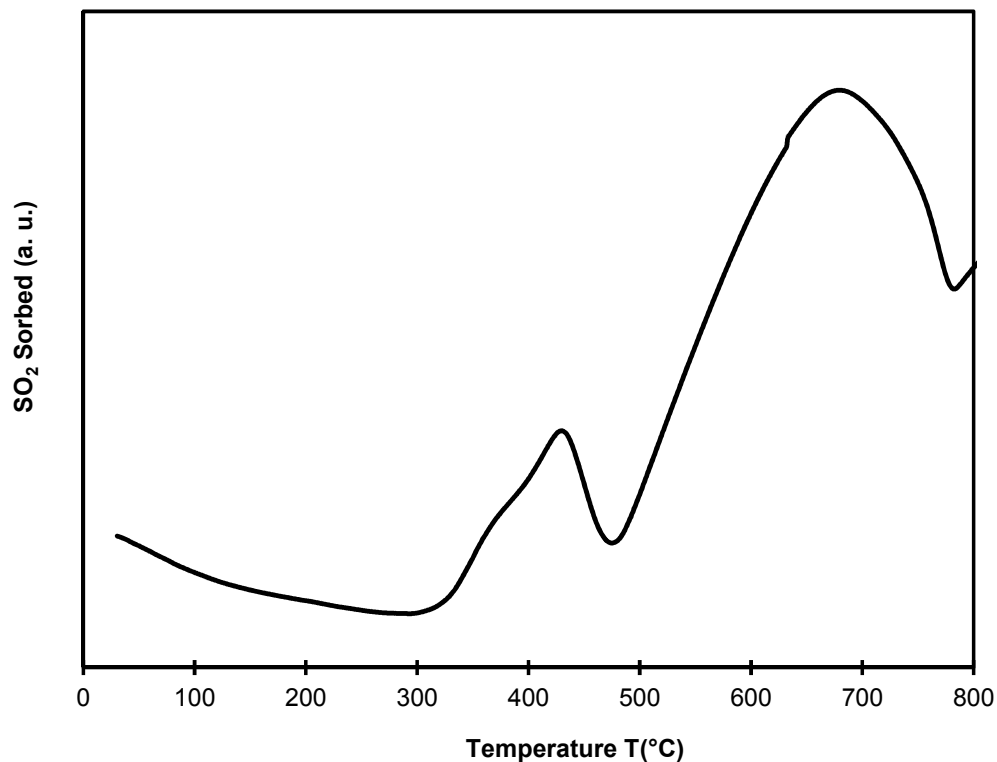
97

98

99 3.2. Effect of temperature in the sorption capacity

100 To determine the temperature interval in which the sorbents were studied, an experiment in the TGA
101 with pure Ca(OH)₂ at heating rate of 10°C/min was performed. The result is shown in Fig. 2. It is
102 observed that the SO₂ sorption process begins at 300°C, and it continues up to 650°C. At temperature
103 interval of 420-480°C is noted a drastic loss of weight, but it can be assigned to Ca(OH)₂
104 decomposition to form CaO, which is also active for adsorbing SO₂. Finally, the selected temperature

105 interval was 350-450°C since at this temperature interval the flue gases enter and exit the preheaters
106 in a thermal power plant, and the proposed technology would be installed at this point.
107



108
109 **Fig. 2. Thermogravimetric profiles of pure Ca(OH)₂ in the sulfurization process at variable**
110 **temperature.**

111 Experiments were carried out at constant temperature for 90 min and the amount of SO₂ sorbed in the
112 prepared materials is presented in Fig. 3. It is clearly noticed that as the temperature increases, the
113 sorption capacity of the materials is enhanced. This effect is observed in all materials regardless of
114 the support, Ca load, or preparation method.
115
116

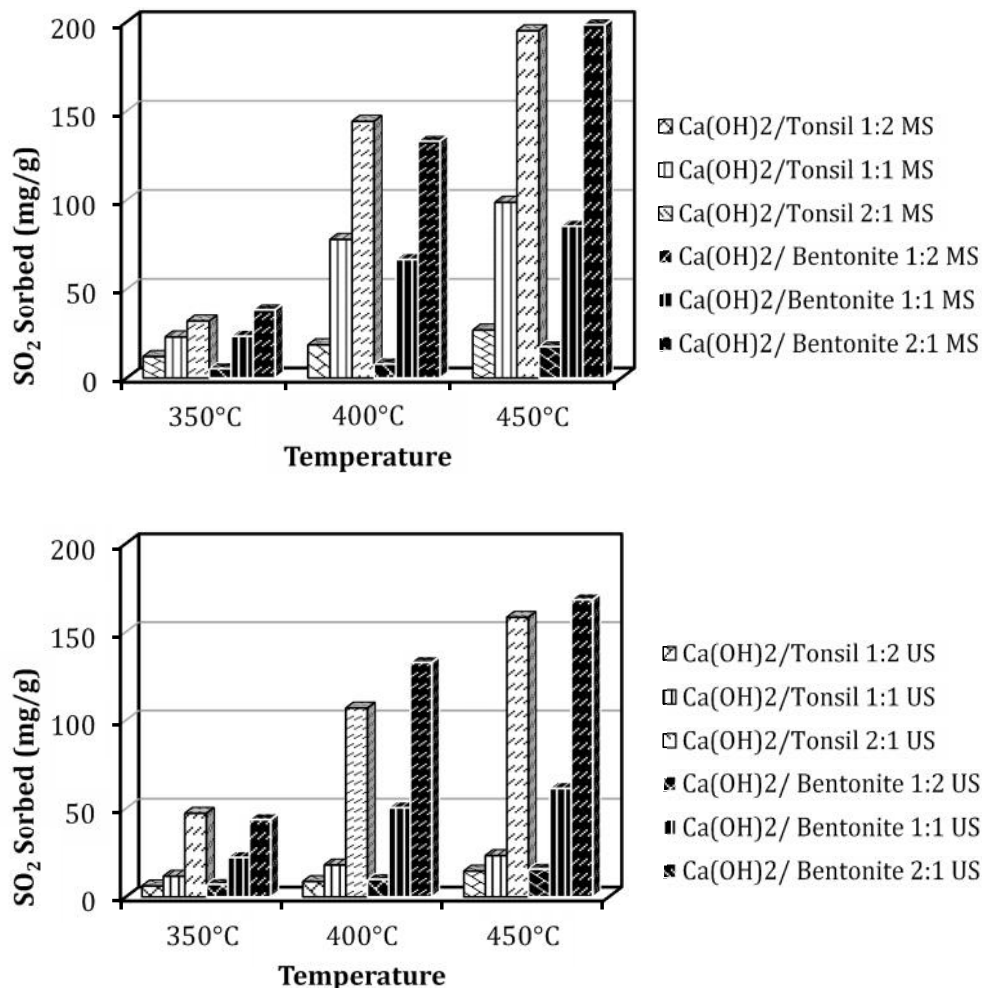


Fig. 3. SO₂ sorption capacity of the different prepared materials at 90 min.

3.3. Effect of calcium load

According to the results presented in Fig. 4, Ca load plays an important role in the sorption capacity of the prepared materials as it has been previously reported [Liu et al., 2004; Macias-Perez et al., 2007; Lin et al., 2003]. At lower temperature (350°C) the effect is not well-defined, but as the temperature increases it is observed that Ca load enhances this property. For instance, at 450°C, and considering the material supported on tonsil and prepared with mechanical stirring, at Ca load of 31 wt%, the sorption capacity is 27 mg/g, but as the Ca load increases to 52 wt% (1.7 times), the sorption capacity rises up to 98 mg/g, which is 3.6 times more than at 31 wt%. Moreover, when Ca load is 68 wt% (1.3 times with respect to the last load), the sorption capacity increases 2 times compared to the last load, sorbing 194 mg/g. These results are unexpected; it seems that supports (either tonsil or bentonite) are blocking the active sites instead of providing better dispersion and more active sites. Similar results were previously reported in materials supported on fly ash at low Ca loads [27].

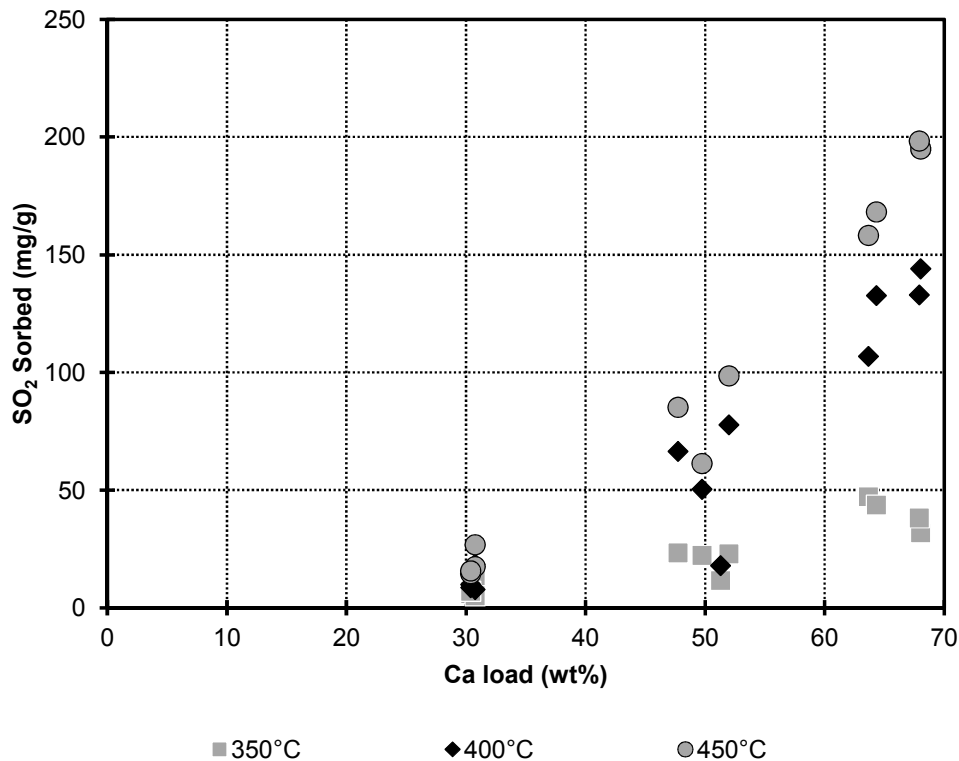


Fig. 4. Effect of calcium load in the SO₂ sorption capacity of the prepared materials.

3.4. Effect of support

The type of support did not show a trend, considering the results presented in Fig. 3. Data suggest that at low Ca loads the materials supported on tonsil result in slightly better yields, but as temperature and Ca load increased this tendency disappears, and finally, at higher temperature (450°C) and Ca load, the better performance was obtained for the material supported on bentonite regardless of preparation method.

3.5. Effect of preparation method

Ultrasonic energy was used trying to improve the yield of the proposed materials. Since the application of ultrasonic materials in slurries is able to fragment the solid particles, decreasing their size, it is proposed that this event would multiply the number of available active sites for the SO₂ sorption process. Nevertheless, the results presented in Fig. 3 do not show an improvement in the performance of the prepared materials. In fact, it is observed that the efficiency of the materials declines when ultrasonic energy is applied during their preparation. This result is attributed to a fusion of the Ca particles when they collide during the application of ultrasonic energy. One of the theories of the particle fragmentation during ultrasonic energy application explains that particles in the slurry are accelerated, and when a collision occurs, they break. Nevertheless, in soft materials, which would be the case of Ca(OH)₂, when the collision happens, the particles are fused, so the particle size increases, and in the case of the present work, would diminish the available active size for the SO₂ sorption process.

3.6. Kinetics parameter estimation

Several models have been developed to represent the heterogeneous non-catalytic solid-gas reaction; however, the most popular used to describe the sulfation of solid sorbents are based on the shrinking core process [28-33]. In this model, it is considered that a first-order chemical reaction between the SO₂ and the calcium core of a spherical particle happens first in the outside surface of the particle forming CaSO₃/CaSO₄. Then, the reaction zone is moved inside the sorbent, leaving behind a converted material and inert solid called "ash" that gradually expands blocking and plugging

167 the pores of the sorbent material because the molar volume of $\text{CaSO}_3/\text{CaSO}_4$ is higher than that of
 168 CaO or $\text{Ca}(\text{OH})_2$. In this way, there is an inert layer shrinking during the chemical reaction. The
 169 relationship between the time and the covered fraction depends on the rate-limiting step. In order for
 170 the reaction to proceed, the SO_2 has to diffuse into the new layer, and it has been shown that rate-
 171 limiting step for sulfur uptake is the diffusion of SO_2 through the pores of the new product layer on the
 172 particle surface [34]. Therefore, the kinetics model that represents the SO_2 sorption process is

$$\frac{t}{k} = \left[3 - 3(1 - \theta)^{2/3} - 2(1 - \theta) \right]$$

$$k = \frac{\rho_B \cdot R^2}{6 \cdot b \cdot \mathcal{D}_e \cdot C_g}$$

173 Where: θ is the covered fraction, ρ_B is the molar density of the active sites in the solid, b is the molar
 174 ratio of solid reactant to gas reactant (ratio of stoichiometric coefficient), R is the radius of unreacted
 175 core, k is the kinetics constant for the surface reaction, C_g is the SO_2 concentration in the flue gas, \mathcal{D}_e
 176 is the effective diffusion coefficient of SO_2 through the “ash”.

177 To improve the adjustment, it was assumed that the SO_2 effective diffusion coefficient, \mathcal{D}_e , depends on
 178 the conversion since the new product layer modifies the SO_2 diffusion characteristics through the
 179 sorbent material:

$$\mathcal{D}_e = \mathcal{D}_{e0} \cdot \left[1 + \alpha_1 e^{(-\alpha_2 \cdot \theta)} \right]$$

180 Non-linear regression analysis was performed using Polymath™ to determine the kinetics parameters
 181 and the results are shown in Tables 2 and 3. According to these results, a good fit was obtained since
 182 the R^2_{adj} was high, and with a few exceptions, it was greater than 0.99. Fig. 5 and 6 present the fit
 183 between the experimental data and the proposed model.

184

185 **Table 2. Kinetics parameters for the SO_2 sorption process in the sorbent materials supported**
 186 **on tonsil.**

187

Material	T [°C]	k [min ⁻¹]	α_1	α_2	R^2_{adj}
Ca-Tonsil 1:2 MS	350	20030	4.304	-13.794	0.9958
	400	7857.592	4.717	-7.582	0.9993
	450	3557.349	11.494	3.899	0.9990
Ca-Tonsil 1:2 UE	350	93860	15.690	49.632	0.9772
	400	25030	22.191	24.597	0.9937
	450	10100	35.430	28.270	0.9897
Ca-Tonsil 1:1 MS	350	10360	6.403	-6.203	0.9982
	400	410.751	1.917	-17.643	0.9981
	450	183.535	0.521	-17.957	0.9983
Ca-Tonsil 1:1 UE	350	33790	7.029	-17.333	0.9938
	400	29330	6.512	8.704	0.9992
	450	11630	8.030	1.545	0.9984
Ca-Tonsil 2:1 MS	350	20320	0.167	-69.655	0.9950
	400	1096.550	4.715×10^{-6}	-56.786	0.9971
	450	637.864	1.357×10^{-8}	-59.974	0.9930
Ca-Tonsil 2:1 UE	350	8256.339	0.073	-52.494	0.9967
	400	2336.802	0.001	-41.779	0.9996
	450	788.094	2.927×10^{-5}	-39.500	0.9694

188

189

190

191

192

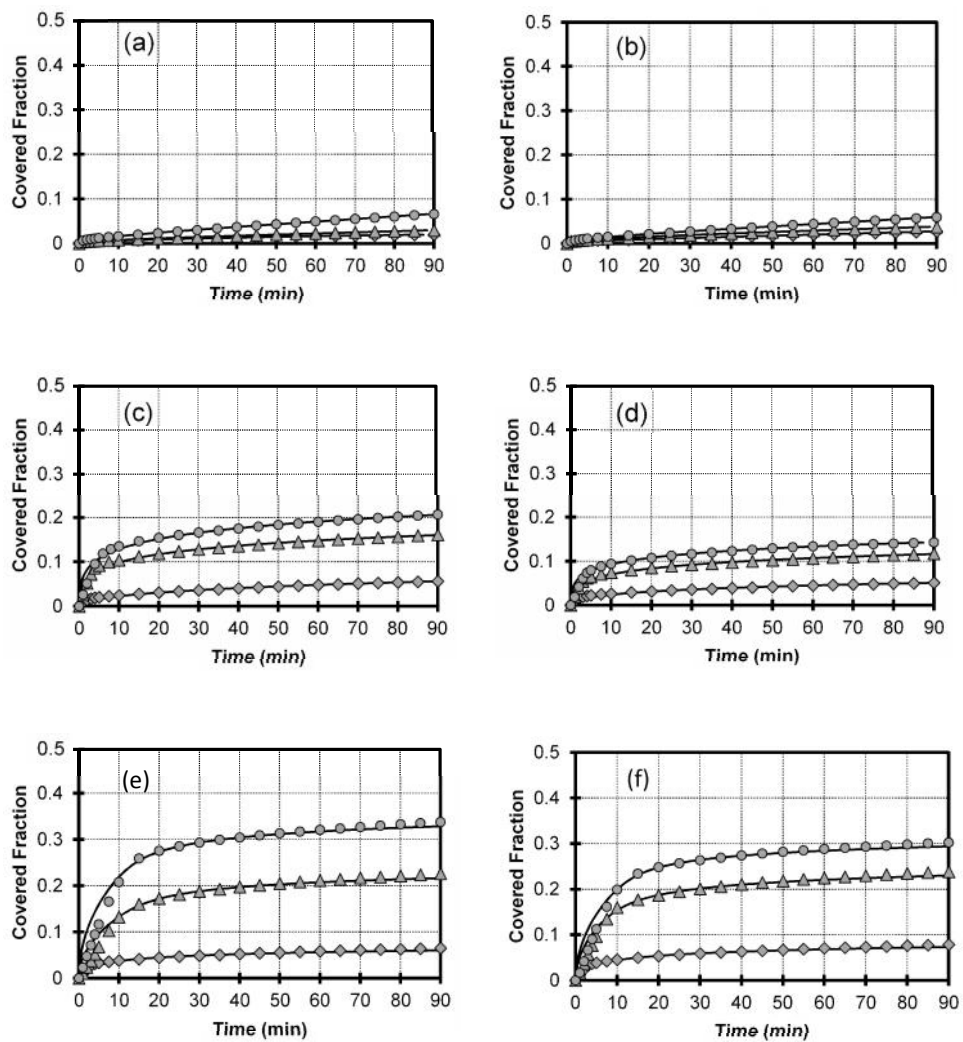
193

194

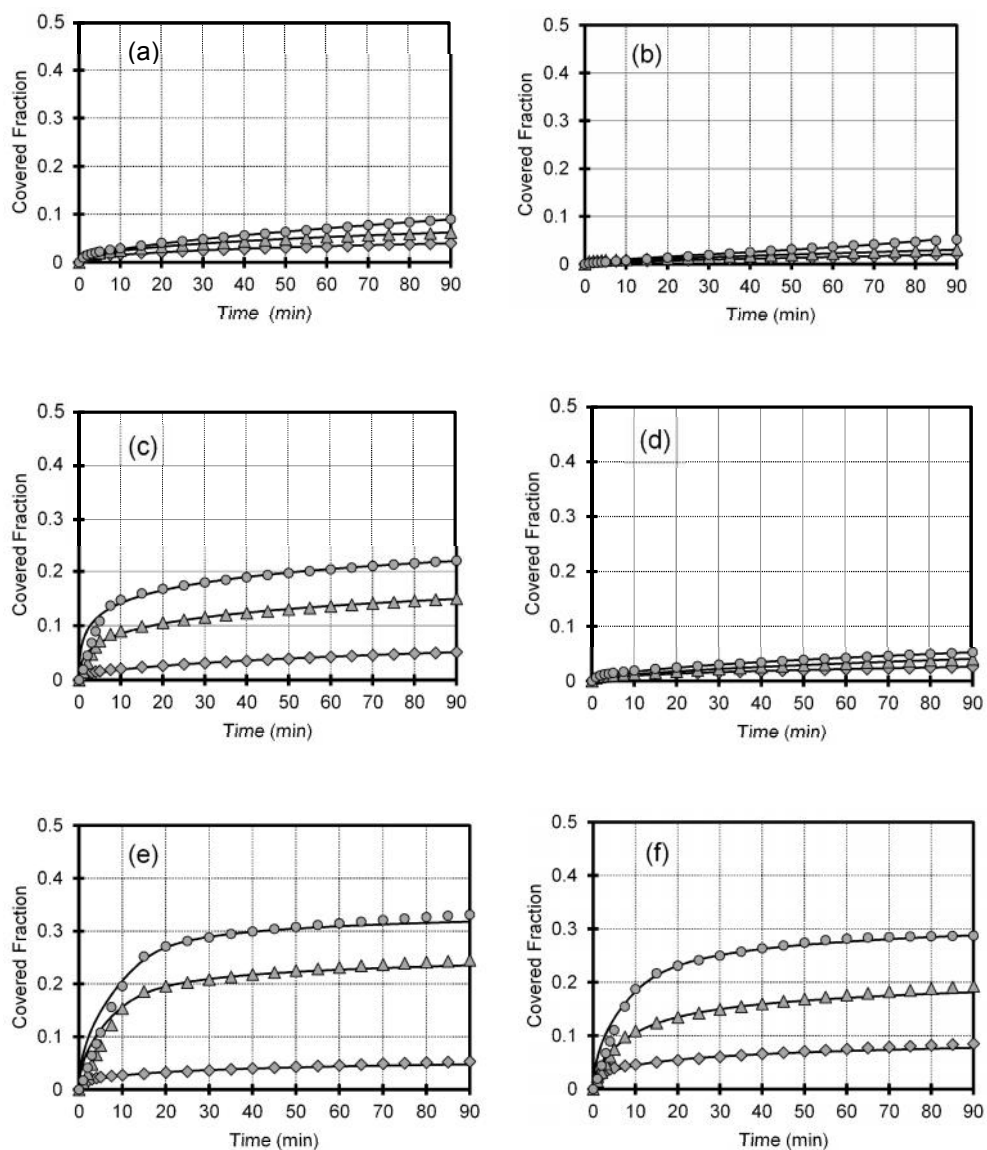
195 **Table 3. Kinetics parameters for the SO₂ sorption process in the sorbent materials supported**
 196 **on bentonite.**
 197

Material	T [°C]	k [min ⁻¹]	A ₁	α ₂	R ² _{adj}
	350	118000	5.989	12.577	0.9961
Ca-Bentonite 1:2 MS	400	43120	13.700	28.002	0.9986
	450	17260	7.5045	16.996	0.9990
	350	159400	5.243	52.851	0.9958
Ca-Bentonite 1:2 UE	400	39910	7.447	19.008	0.9992
	450	14130	11.815	17.397	0.9995
	350	1978.496	22.534	-10.788	0.9987
Ca-Bentonite 1:1 MS	400	170.806	2.150	-20.357	0.9980
	450	89.447	2.234	-16.238	0.9977
	350	3207.537	8.1381	-25.955	0.9960
Ca-Bentonite 1:1 UE	400	231.918	3.984	-25.851	0.9973
	450	114.568	2.374	-26.532	0.9984
	350	12890	0.028	-85.340	0.9975
Ca-Bentonite 2:1 MS	400	1549.378	1.818×10 ⁻⁵	-54.394	0.9965
	450	542.590	2.99×10 ⁻⁶	-41.960	0.9946
	350	8784.110	0.037	-65.092	0.9982
Ca-Bentonite 2:1 UE	400	1075.256	7.904×10 ⁻⁵	-46.198	0.9985
	450	666.017	1.171×10 ⁻⁶	-50.314	0.9956

198
 199 To determine the dependency of the diffusion coefficient, \mathcal{D}_{e0} , with respect to temperature, it is
 200 necessary to point out that it cannot be directly determined because ρ_B and R , which are other
 201 physical parameters involved in k , were not experimentally determined. However, some trends with
 202 respect to temperature, support, and preparation method are detected. First, it is critically important to
 203 emphasize that if the numerical value of k decreases, it implies that \mathcal{D}_{e0} increases since the other
 204 parameters are constant, and vice versa, an increase of k means a reduction in the diffusion
 205 coefficient. It is observed that in all the prepared materials (regardless the support, Ca load, or
 206 preparation method) as temperature increases the value of \mathcal{D}_{e0} also raises. So, an Arrhenius-type
 207 dependence with respect to temperature can be obtained. Activation energy was calculated and is
 208 presented in Tables 4 and 5. At low Ca loads the activation energy of material supported on tonsil is
 209 smaller compared to those supported on bentonite; however, when increasing the Ca load, the
 210 activation energy of material supported on bentonite is less when ultrasonic energy is applied during
 211 preparation method. This confirms the previous statement that materials supported on bentonite give
 212 better results as the Ca load and temperature augments.
 213



214
 215 **Fig. 5. Adjustment of the experimental data to the kinetics proposed model for Ca(OH)_2**
 216 **supported on bentonite: \blacklozenge 350°C, \blacktriangle 400°C, \bullet 450°C. (a) MS 1:2; (b) UE 1:2; (c) MS 1:1; (d) UE**
 217 **1:1; (e) MS 2:1; (f) UE 2:1**
 218
 219
 220
 221
 222
 223
 224
 225
 226
 227
 228



229
230
231
232
233
234
235
236

Fig. 6. Adjustment of the experimental data to the kinetics proposed model for $\text{Ca}(\text{OH})_2$ supported on tonsil: \blacklozenge 350°C, \blacktriangle 400°C, \bullet 450°C. (a) MS 1:2; (b) UE 1:2; (c) MS 1:1; (d) UE 1:1; (e) MS 2:1; (f) UE 2:1

Table 4. Activation energy for the SO_2 sorption process in materials supported on tonsil.

Material	E_A/R [K^{-1}]
Ca-Tonsil 1:2 MS	$7,789.5 \pm 492.31$
Ca-Tonsil 1:2 UE	$10,070.0 \pm 8,203.81$
Ca-Tonsil 1:1 MS	$18,410.0 \pm 7,004.00$
Ca-Tonsil 1:1 UE	$4,710.2 \pm 2,847.00$
Ca-Tonsil 2:1 MS	$15,830.0 \pm 6,998.00$
Ca-Tonsil 2:1 UE	$10,590.0 \pm 26.07$

237
238
239
240

241 **Table 5. Activation energy for the SO₂ sorption process in materials supported on bentonite.**
 242

Material	E _A /R [K ⁻¹]
Ca-Bentonite 1:2 MS	8,656.7 ± 1,705.43
Ca-Bentonite 1:2 UE	10,940.0 ± 5,493.74
Ca-Bentonite 1:1 MS	14,130.0 ± 5,190.00
Ca-Bentonite 1:1 UE	15,200.0 ± 5,525.00
Ca-Bentonite 2:1 MS	14,370.0 ± 2,752.00
Ca-Bentonite 2:1 UE	11,780.0 ± 4,718.00

243

244

245

246

4. CONCLUSION

247

248 Materials based on Ca(OH)₂ and supported on bentonite and tonsil were prepared at different mass
 249 ratios and tested in a thermogravimetric balance to determine their SO₂ sorption capacity. These
 250 materials were active for the desulfurization of flue gases, and their activity was improved as the
 251 calcium load and temperature increased. On the other hand, support was not important since the
 252 activity was almost the same at different experimental conditions; however, at low temperature activity
 253 was slightly better for materials supported on tonsil, but those supported on bentonite gave better
 254 results as the Ca load and temperature increased. When ultrasonic energy was applied during the
 255 preparation of the sorbent materials, their activity decreased, and it was attributed to an
 256 agglomeration of Ca particles, so the available active sites decreased. The SO₂ sorption process was
 257 represented by a modified shrinking core process model, and the kinetics parameters were estimated
 258 using PolymathTM. It was found that the effective diffusion coefficient increased with temperature.
 259 Activation energy of materials supported on bentonite was greater at low Ca load, but as this load
 260 increased, their activation energy was smaller compared to materials supported on tonsil.

261

262

263

REFERENCES

264

- 265 1. Barreca, A. I., Neidell, M. and Sanders, N. J. (2017). Long-Run Pollution Exposure and Adult
 266 Mortality: Evidence from the Acid Rain Program (No. w23524). National Bureau of Economic
 267 Research.
- 268 2. Di Maria, C., Lange, I. and Van der Werf, E. (2014). Should we be worried about the green
 269 paradox? Announcement effects of the Acid Rain Program. *Eur. Econ. Rev.*, 69, 143-162.
- 270 3. Burns, D. A., Aherne, J., Gay, D. A., and Lehmann, C. (2016). Acid rain and its environmental
 271 effects: Recent scientific advances. *Atmos. Environ.*, 146, 1-4.
- 272 4. Chanel, O., Henschel, S., Goodman, P. G., Analitis, A., Atkinson, R. W., Le Tertre, and Medina, S.
 273 (2014). Economic valuation of the mortality benefits of a regulation on SO₂ in 20 European cities.
 274 *Eur. J. Public Health*, 24(4), 631-637.
- 275 5. Raymond, B. A.; Basingthwaite, T.; D. P. (2010). Measuring nitrogen and sulphur deposition in
 276 the Georgia Basin, British Columbia, using lichens and moss, *J. Limnol.*, 69, 22-32.
- 277 6. Rosi-Marshall, E. J., Bernhardt, E. S., Buso, D. C., Driscoll, C. T., and Likens, G. E. (2016). Acid
 278 rain mitigation experiment shifts a forested watershed from a net sink to a net source of nitrogen.
 279 *Proceedings of the National Academy of Sciences*, 113(27), 7580-7583.
- 280 7. Aksoyoglu, S., Keller, J., Ciarelli, G., Prévôt, A. S. H., and Baltensperger, U. (2014). A model study
 281 on changes of European and Swiss particulate matter, ozone and nitrogen deposition between
 282 1990 and 2020 due to the revised Gothenburg protocol. *Atmos. Chem. Phys.*, 14(23), 13081-
 283 13095.
- 284 8. Bento, A., Freedman, M., and Lang, C. (2015). Who benefits from environmental regulation?
 285 Evidence from the clean air act amendments. *Rev. Econ. Stat.*, 97(3), 610-622.
- 286 9. Chestnut, L.G.; Mills, D. M. (2005). A fresh look at the benefits and costs of the US acid rain
 287 program, *J. Environ. Manage.*, 77, 252-266.
- 288 10. Ferris, A. E., Shadbegian, R. J., and Wolverton, A. (2014). The effect of environmental regulation
 289 on power sector employment: Phase I of the Title IV SO₂ trading program. *J. Assoc. Environ.*
 290 *Resour. Econ.*, 1(4), 521-553.
- 291 abatement cost of coal-fired power plants in China. *Energy Policy*, 85, 347-356.

- 292 11. Cheng, J.; Zhou, J.; Liu, J.; Zhou, Z.; Huang, Z.; Cao, X.; Zhao, X.; Cen, K. (2003). Sulfur removal
293 at high temperature during coal combustion in furnaces: A review, *Prog. Energy Combust. Sci.*, 29,
294 381–405.
- 295 12. Du, Y. J., Wei, M. L., Reddy, K. R., Liu, Z. P., and Jin, F. (2014). Effect of acid rain pH on leaching
296 behavior of cement stabilized lead-contaminated soil. *J. Hazard. Mater.*, 271, 131-140.
- 297 13. Srivastava, R.K., Miller, C.A., Erickson, C., and Jambhekar, (2004). R. Emissions of sulfur trioxide
298 from coal-fires power plants, *J. Air Waste Manage. Assoc.*, 54, 750-762.
- 299 14. Chen, H., and Khalili, N. (2017). Fly-Ash-Modified Calcium-Based Sorbents Tailored to CO₂
300 Capture. *Ind. Eng. Chem. Res.*, 56(7), 1888-1894.
- 301 15. Donat, F., and Müller, C. R. (2018). A critical assessment of the testing conditions of CaO-based
302 CO₂ sorbents. *Chem. Eng. J.*, 336, 544-549.
- 303 16. Gong, G.; Ye, S.; Tian, Y.; Cui, Y.; Chen, Y. (2008). Characterization of blast furnace slag-
304 Ca(OH)₂ sorbents for flue gas desulfurization, *Ind. Eng. Chem. Res.*, 47, 7897-7902.
- 305 17. He, D., Shao, Y., Qin, C., Pu, G., Ran, J., and Zhang, L. (2016). Understanding the Sulfation
306 Pattern of CaO-Based Sorbents in a Novel Process for Sequential CO₂ and SO₂ Capture. *Ind.*
307 *Eng. Chem. Res.*, 55(39), 10251-10262.
- 308 18. Karatepe, N.; Erdogan, N.; Ersoy-Mericboyu, A.; Kucukbayrak, S. (2004). Preparation of
309 diatomite/Ca(OH)₂ sorbents and modelling their sulphation reaction, *Chem. Eng. Sci.*, 59, 3883-
310 3889.
- 311 19. Li, T.; Zhuo, Y.; Lei, J.; Xu, X. (2007). Simultaneous removal of SO₂ and NO by low cost sorbent-
312 catalysts prepared by lime, fly ash and industrial waste materials, *Korean J. Chem. Eng.*, 24, 1113-
313 1117.
- 314 20. Macias-Perez, M. C.; Bueno-Lopez, A.; Lillo-Rodenas, M. A.; Salinas-Martinez de Lecea, C.;
315 Linares-Solano, A. (2007). SO₂ retention on CaO/activated carbon sorbents. Part I: Importance of
316 calcium loading and dispersion, *Fuel*, 86, 677–683.
- 317 21. Renedo, M. J., Gonzalez, F.; Pesquera, C.; Fernandez, J. (2006). Study of sorbents prepared
318 from clays and CaO or Ca(OH)₂ for SO₂ removal at low temperature, *Ind. Eng. Chem. Res.*, 45,
319 3752-3757.
- 320 22. Bartos, C., Kukovecz, Á., Ambrus, R., Farkas, G., Radacsi, N., and Szabó-Révész, P. (2015).
321 Comparison of static and dynamic sonication as process intensification for particle size reduction
322 using a factorial design. *Chem. Eng. Process. Process Intensif.*, 87, 26-34.
- 323 23. Bukhari, S. S., Behin, J., Kazemian, H., and Rohani, S. (2015). Conversion of coal fly ash to
324 zeolite utilizing microwave and ultrasound energies: a review. *Fuel*, 140, 250-266.
- 325 24. Kotadia, H. R., and Das, A. (2015). Modification of solidification microstructure in hypo-and hyper-
326 eutectic Al–Si alloys under high-intensity ultrasonic irradiation. *J. Alloys Compd.*, 620, 1-4.
- 327 25. Lim, W. T. L.; Zhong, Z.; Borgna, A. (2009). An effective sonication-assisted reduction approach to
328 synthesize highly dispersed Co nanoparticles on SiO₂, *Chem. Phys. Lett.*, 471, 122-127.
- 329 26. Poli, A. L.; Batista, T.; Schmitt, C. C.; Gessner, F.; Neumann, M. G. (2008). Effect of sonication on
330 the particle size of montmorillonite clays, *J. Colloid. Interface Sci.*, 325, 386-390.
- 331 27. Lin, R. B., Shih, S. M., and Liu, C. F. (2003). Structural properties and reactivities of Ca(OH)₂/fly
332 ash sorbents for flue gas desulfurization, *Ind. Eng. Chem. Res.*, 42, 1350-1356.
- 333 Liu, C.F., Shih, S.M., and Lin, R.B. (2004). Effect of Ca(OH)₂/fly ash weight ratio on the kinetics of the
334 reaction of Ca(OH)₂/fly ash sorbents with SO₂ at low temperatures, *Chem. Eng. Sci.*, 59, 4653-
335 4655.
- 336 28. Bahrin, D., Subagjo, S., and Susanto, H. (2016). Kinetic study on the SO₂ adsorption using
337 CuO/γ-Al₂O₃ adsorbent. *Bull. Chem. React. Eng. Catal.*, 11(1), 93-99.
- 338 29. Lee, K. T., and Koon, O. W. (2009). Modified shrinking unreacted-core model for the reaction
339 between sulfur dioxide and coal fly ash/CaO/CaSO₄ sorbent, *Chem. Eng. J.*, 146, 57–62.
- 340 30. Lv, L., Yang, J., Shen, Z., Zhou, Y., & Lu, J. (2017). Effect of additives on limestone reactivity in
341 flue gas desulfurization. *Energy Sources Part A*, 39(2), 166-171.
- 342 31. Renedo, M. J., and Fernandez, J. (2004). Kinetic modelling of the hydrothermal reaction of fly ash,
343 Ca(OH)₂ and CaSO₄ in the preparation of desulfurant sorbents. *Fuel*, 83(4-5), 525-532.
- 344 32. Wang, J., Guo, J., Parnas, R., and Liang, B. (2015). Calcium-based regenerable sorbents for high
345 temperature H₂S removal. *Fuel*, 154, 17-23.
- 346 33. Yang, Q., and Lin, Y.S. (2006). Kinetics of carbon dioxide sorption on perovskite-type metal
347 oxides. *Ind. Eng. Chem. Res.*, 45, 6302-6310.
- 348 34. Zhao, R., Liu, H., Ye, S., Xie, Y., and Chen, Y. (2006). Ca-based sorbents modified with humic
349 acid for flue gas desulfurization, *Ind. Eng. Chem. Res.*, 45, 7120-7125.